

Cross sections and Rosenbluth separations in ${}^1\text{H}(e, e'\text{K}^+)\Lambda$ up to $Q^2=2.35 \text{ GeV}^2$

M. Coman,¹ P. Markowitz,¹ K.A. Aniol,² K. Baker,³ W.U. Boeglin,⁴ H. Breuer,⁴ P. Bydžovský,⁵ A. Camsonne,⁶ J. Cha,³ C.C. Chang,⁴ N. Chant,⁴ J.-P. Chen,⁷ E.A. Chudakov,⁷ E. Cisbani,⁸ L. Cole,³ F. Cusanno,⁸ C.W. de Jager,⁷ R. De Leo,⁹ A.P. Deur,¹⁰ S. Dieterich,¹¹ F. Dohrmann,¹² D. Dutta,¹³ R. Ent,⁷ O. Filoti,¹⁴ K. Fissum,¹³ S. Frullani,¹⁴ F. Garibaldi,¹⁴ O. Gayou,¹³ F. Gilman,¹¹ J. Gomez,⁷ P. Gueye,³ J.O. Hansen,⁷ D.W. Higinbotham,⁷ W. Hinton,³ T. Horn,⁴ B. Hu,¹⁵ G.M. Huber,¹⁵ M. Iodice,¹⁶ C. Jackson,³ X. Jiang,¹¹ M. Jones,¹⁷ K. Kanda,¹⁸ C. Keppel,³ P. King,⁴ F. Klein,¹⁹ K. Kozlov,¹⁵ K. Kramer,¹⁷ L. Kramer,¹⁹ L. Lagamba,⁹ J.J. LeRose,⁷ N. Livanage,⁷ D.J. Margaziotis,² S. Marrone,⁹ K. McCormick,¹¹ R.W. Michaels,⁷ J. Mitchell,⁷ T. Miyoshi,¹⁸ S. Nanda,⁷ M. Palomba,⁹ V. Pattichio,⁹ C.F. Perdrisat,²⁰ E. Piassetzky,²¹ V.A. Punjabi,²² B. Raue,¹ J. Reinhold,¹ B. Reitz,⁷ R.E. Roche,²³ P. Roos,⁴ A. Saha,⁷ A.J. Sarty,²³ Y. Sato,¹⁸ S. Širca,¹³ M. Sotona,⁵ L. Tang,³ H. Ueno,²⁴ P.E. Ulmer,²⁵ G.M. Urciuoli,⁸ A. Uzzle,²⁵ A. Vacheret,²⁶ K. Wang,¹⁰ K. Wijesooriya,¹² B. Wojtsekhowski,⁷ S. Wood,⁷ I. Yaron,²¹ X. Zheng,¹³ and L. Zhu¹³

(Jefferson Lab Hall A Collaboration)

¹Florida International University, Miami, Florida 33199, USA

²California State University, Los Angeles, Los Angeles, California 90032, USA

³Hampton University, Hampton, Virginia 23668, USA

⁴University of Maryland, College Park, Maryland 20742, USA

⁵Nuclear Physics Institute, Řež near Prague, Czech Republic

⁶Université Blaise Pascal/IN2P3, F-63177 Aubière, France

⁷Thomas Jefferson National Accelerator Facility, Newport News, Virginia 23606, USA

⁸Istituto Nazionale di Fisica Nucleare, Sezione di Roma1, Piazza A. Moro, Rome, Italy

⁹Istituto Nazionale di Fisica Nucleare, Sezione di Bari and University of Bari, I-70126 Bari, Italy

¹⁰University of Virginia, Charlottesville, Virginia 22904, USA

¹¹Rutgers, The State University of New Jersey, Piscataway, New Jersey 08855, USA

¹²Argonne National Laboratory, Argonne, Illinois 60439, USA

¹³Massachusetts Institute of Technology, Cambridge, Massachusetts 02139, USA

¹⁴Istituto Nazionale di Fisica Nucleare, Sezione di Roma1,

gruppo collegato Sanità, and Istituto Superiore di Sanità, I-00161 Roma, Italy

¹⁵University of Regina, Regina, SK, S4S-OA2, Canada

¹⁶Istituto Nazionale di Fisica Nucleare, Sezione di Roma Tre, I-00146 Roma, Italy

¹⁷The College of William and Mary in Virginia, Williamsburg, Virginia 23187, USA

¹⁸Tohoku University, Sendai, 980-8578, Japan

¹⁹Florida International University, Miami Florida, 33199

²⁰College of William and Mary, Williamsburg, Virginia 23187, USA

²¹School of Physics and Astronomy, Sackler Faculty of Exact Science, Tel Aviv University, Tel Aviv 69978, Israel

²²Norfolk State University, Norfolk, Virginia 23504, USA

²³Florida State University, Tallahassee, Florida 32306, USA

²⁴Yamagata University, Yamagata 990-8560, Japan

²⁵Old Dominion University, Norfolk, Virginia 23508, USA

²⁶Daphnia/SPhN, CEN Saclay, 91191 Gif-sur-Yvette Cedex, France

(Dated: October 9, 2018)

The kaon electroproduction reaction ${}^1\text{H}(e, e'\text{K}^+)\Lambda$ was studied as a function of the virtual-photon four-momentum, Q^2 , total energy, W , and momentum transfer, t , for different values of the virtual-photon polarization parameter. Data were taken at electron beam energies ranging from 3.40 to 5.75 GeV. The center of mass cross section was determined for 21 kinematics corresponding to Q^2 of 1.90 and 2.35 GeV^2 and the longitudinal, σ_L , and transverse, σ_T , cross sections were separated using the Rosenbluth technique at fixed W and t . The separated cross sections reveal a flat energy dependence at forward kaon angles not satisfactorily described by existing electroproduction models. Influence of the kaon pole on the cross sections was investigated by adopting an off-shell form factor in the Regge model which better describes the observed energy dependence of σ_T and σ_L .

PACS numbers: xxxxx

Understanding the structure of nuclei and the interaction between nucleons in terms of sub-nucleonic degrees of freedom (quarks and gluons) is the goal of intermediate-energy nuclear physics. The advantage of

electron scattering is that the one-photon exchange is a good approximation and can be calculated precisely [1]. This allows factorization of the electron and hadron dynamics in the electroproduction cross section. It is gen-

erally accepted that at four momentum transfers, $Q^2 \geq 1$ GeV², the virtual photon probes the sub-nucleonic structure of the hadron (see e.g. [2]). Electron beams in the energy range used at the Thomas Jefferson National Accelerator Facility (JLab) therefore can access the sub-nucleonic structure of hadrons. However, these energies probe only nonperturbative aspects of QCD. In the nonperturbative region, effective hadronic models play an essential role and experimental testing is crucial in understanding the underlying physics of hadron electroproduction. The JLab program on electromagnetic strangeness production is of particular interest due to the presence of the additional strange flavour degree of freedom. High-precision data from experiments on kaon electroproduction[3, 4] let current models (e.g. the Saclay-Lyon [5] and Regge [6] models) be refined (fitting parameters and revising underlying assumptions).

The cross section of the exclusive $^1\text{H}(e, e'K^+)\Lambda$ reaction with unpolarized electrons can be expressed in terms of the $\gamma^* + p \rightarrow K^+ + \Lambda$ virtual photoproduction binary-process cross section as:

$$\frac{d^5\sigma}{dE'_e d\Omega_e d\Omega_K} = \Gamma \frac{d\sigma(\gamma^*, K)}{d\Omega_K} \quad (1)$$

Γ being the virtual photon flux.

In turn, the center-of-mass virtual photoproduction cross section can be expressed via four separated cross sections:

$$\frac{d\sigma(\gamma^*, K)}{d\Omega_K} = \sigma_T + \epsilon\sigma_L + \epsilon\sigma_{TT} \cos 2\Phi + \sqrt{2\epsilon(\epsilon+1)}\sigma_{LT} \cos \Phi \quad (2)$$

where $\epsilon = 1/[1 + 2|\vec{q}|^2/Q^2 \tan^2(\vartheta_e/2)]$ is the photon polarization parameter, and Φ is the angle between the leptonic plane (defined by the incoming and outgoing electrons), and reaction plane (defined by the virtual-photon and kaon 3-momenta).

The terms in eq.(2) correspond to the cross section for transverse (σ_T), longitudinal (σ_L), transverse-transverse interference (σ_{TT}) and longitudinal-transverse interference (σ_{LT}) kaon production by virtual photons. They only depend on the variables Q^2 ($= -q^2$, the squared virtual-photon 4-momentum), W (the photon-nucleon center of mass energy) and t (the squared 4-momentum transfer to the kaon).

In ‘‘parallel’’ kinematics (the virtual-photon and kaon 3-momenta are parallel), the interference terms vanish, allowing the separation of the longitudinal and transverse parts with the Rosenbluth technique.

The results from the E98-108 experiment [7] in Hall A at Jefferson Lab presented in this letter provide new information on the behavior of the separated cross sections of the $^1\text{H}(e, e'K^+)\Lambda$ exclusive reaction in an unexplored region of Q^2 , W , and t where no separations have been performed.

The E98-108 data were taken using the JLab continuous electron beam with currents as high as 100 μA . The

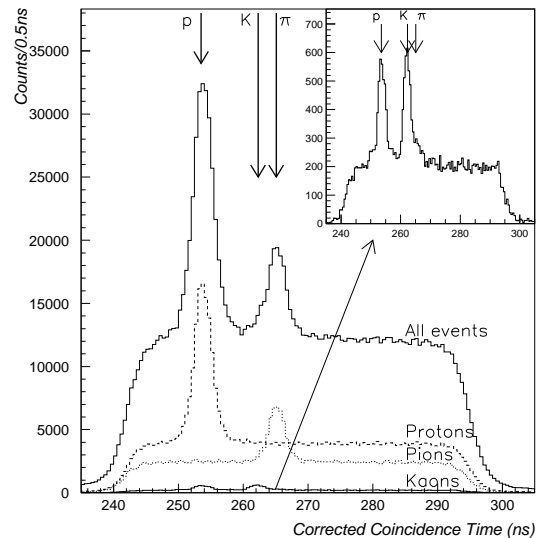


FIG. 1: Electron-hadron coincidence time spectra with different aerogel-counter based hadron selection. See the text for further explanation.

beam was scattered off a 15 cm, cryogenic liquid hydrogen target (LH₂). Background distributions from the aluminum windows were obtained from an empty target cell replica. The scattered electrons and kaons were detected in coincidence in two High Resolution Spectrometers (HRS)[8]. The HRSs can achieve a momentum resolution of 2×10^{-4} and an angular resolution of about 2 mrad.

To perform particle identification (PID) of the knock-out kaons, two new aerogel detectors [8, 9, 10], were built and installed in the hadron arm to provide kaon identification in the measured range of momenta, from 1.7 to 2.6 GeV/c. The counter with lower refractive index ($n=1.015$) detected pions, while the higher index counter ($n=1.055$) detected both pions and kaons. Information from the two detectors was combined to identify pions, kaons and protons. Figure 1 shows the coincidence time spectrum between the electron and hadron arm. Without any PID cut the spectrum is dominated by protons (identified by neither aerogel firing) and pions (identified by both aerogels firing), kaons amounting only to a small fraction of the produced hadrons. The exploded part, showing kaon events (identified by the first detector not firing and the second detector firing), shows the kaon peak and the suppression of the pion peak. A fraction of protons leak through the selection by producing Cherenkov light via electron knock-on processes.

Figure 2 shows the reconstructed mass, M_x , of the unobserved baryon in the $^1\text{H}(e, e'K^+)\Lambda$ reaction, in this case either a Λ or a Σ^0 hyperon. Accidental coincidences were subtracted using a side-band in the timing window. The present analysis is limited to the exclusive $K^+-\Lambda$

production channel, *e.g.* $1105.0 < M_x < 1155.0$ MeV/c².

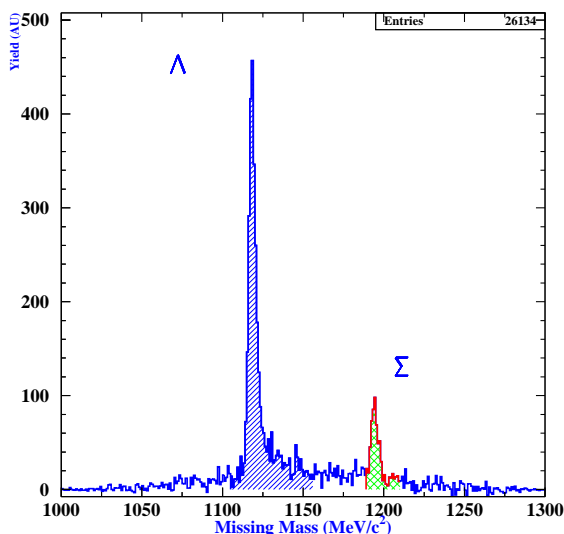


FIG. 2: Λ and Σ missing mass spectra obtained at $Q^2=1.9$ GeV². The region of integration is highlighted.

Kaon electroproduction was measured at 21 different kinematic settings. The $\frac{d^5\sigma}{dE'_e d\Omega_e d\Omega_K}$ cross section was determined by comparing the measured yield (corrected for detector inefficiencies) with the simulated yield from the Monte Carlo for $(e, e'p)$ reactions (MCEEP) program[11], extended to kaon electroproduction. MCEEP also was used to determine the correction for kaon survival (which varied between 15-27%) and the radiative correction (which varied between 1.04 and 1.12). MCEEP uses a model for kaon electroproduction based on [12] updated as in [13] to account for cross section variation across the kinematic acceptance and to extract both the acceptance averaged and point acceptance $\frac{d\sigma(\gamma^*, k)}{d\Omega_K}$.

The separation of the longitudinal and transverse cross sections was done using the point cross sections for kaons detected along the direction of the virtual photon at different values of the virtual photon polarization parameter ϵ , but keeping Q^2 , W and t simultaneously constant (*e.g.*, a Rosenbluth separation). The $^1\text{H}(e, e'K^+)\Lambda$ cross sections are reported in Table I. The systematic uncertainties associated with the cross sections are presented in Table II. The total systematic uncertainty in the cross section amounts to 2.8%. Details of the analysis are in [14].

The experiment provides the first good quality separated transverse and longitudinal cross sections as a function of energy. In the studied kinematical region the cross sections reveal a flat and almost constant energy dependence suggesting a quite steep rise of the cross sections in the threshold region. The longitudinal cross sections are evidently (due to their relatively small error bars) non zero in agreement with the rise of σ_L as a

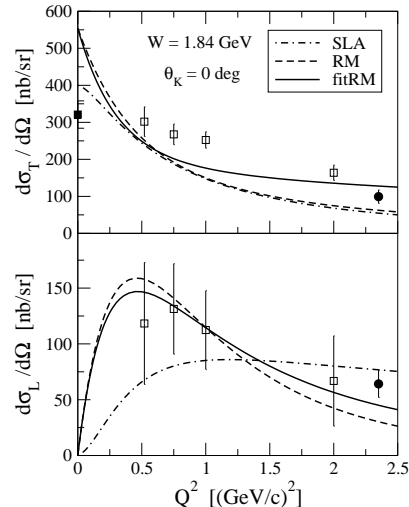


FIG. 3: Separated cross sections from this experiment (full circle) and [4] (squares) as a function of Q^2 at $W = 1.84$ GeV and zero kaon scattering angle in comparison with predictions of the models (see the text for discussion of the curves). The photoproduction point (full square) is from Ref. [15].

function of energy observed by [3] for smaller Q^2 . The data are also consistent with those by [4], see Fig. 3.

The data are shown in Figs. 3 and 4 compared to the isobar Saclay-Lyon (SLA) [5] and Regge (RM) [6] model calculations. Both models systematically underpredict σ_T , but give the flat energy dependence observed (Fig. 4). The models give different results for σ_L . The RM model reproduces the Q^2 -dependence of σ_L but not the flat energy dependence seen in Fig. 4 b and d. The new data provide information necessary to refine the models and understand the dynamics of the process. A similar inability of the current models to describe recent data was also shown in Ref. [3].

The flat energy dependence of the cross sections at forward kaon angles suggests the reaction mechanism is dominated by the non-resonant t -channel contribution seen also in photoproduction [16, 17]. The Regge model was modified to take into account possible off-mass-shell effects by assuming a more complex phenomenological prescription for the electromagnetic form factors of the exchanged K and K* mesons:

$$F_x(Q^2, t) = \Lambda_x^2 / (\Lambda_x^2 + Q^2) + c_x (m_x^2 - t) Q^2 / (\Lambda_x^2 + Q^2)^2 \quad (3)$$

($x = K$ and K^*). $\Lambda_K^2 = 0.7$ (GeV/c)² and $\Lambda_{K^*}^2 = 0.6$ (GeV/c)² were fixed to reproduce mean-square electromagnetic charge radii of both mesons from previous low Q^2 data on the kaon form factor[18].

The second term in eq. (3) is the off-mass-shell first-order correction in t near the pole. The prescription does not violate gauge invariance since in the RM the basic operator being multiplied by the off-shell form factor is already gauge invariant [6].

The parameters c_x were fit to $c_x = 0.87$ and 0.79 for K and K*, from a least square fit to the new data and

TABLE I: Unseparated and separated transverse and longitudinal cross sections for the $p(e, e'K^+)\Lambda$ reaction as measured in E98-108 experiment. E_0 is the beam energy. Errors are statistical for the unseparated and total (statistical and systematical combined in quadrature) for separated cross sections.

$Q^2 = 1.90 \text{ (GeV/c)}^2$						
E_0	W	t	ϵ	$\sigma_T + \epsilon\sigma_L$	σ_L	σ_T
[GeV]	[GeV]	[(GeV/c) ²]		[nb/sr]	[nb/sr]	[nb/sr]
5.754	1.91	-0.5994	0.811	177.6 ± 8.6	65.0 ± 11.6	125.5 ± 17.0
4.238		-0.6183	0.637	170.7 ± 11.6		
3.401		-0.6183	0.401	149.7 ± 11.5		
5.614	1.94	-0.5790	0.800	178.9 ± 5.9	56.4 ± 6.8	134.2 ± 10.5
4.238		-0.5790	0.613	170.0 ± 7.5		
3.401		-0.5790	0.364	154.4 ± 7.0		
5.754	2.00	-0.5203	0.792	171.8 ± 7.1	80.5 ± 15.9	108.0 ± 23.0
4.238		-0.5203	0.575	162.7 ± 7.4		
5.614	2.14	-0.4143	0.726	161.4 ± 5.4	36.9 ± 14.3	134.6 ± 21.3
4.238		-0.4143	0.471	152.1 ± 9.4		
$Q^2 = 2.35 \text{ (GeV/c)}^2$						
E_0	W	t	ϵ	$\sigma_T + \epsilon\sigma_L$	σ_L	σ_T
[GeV]	[GeV]	[(GeV/c) ²]		[nb/sr]	[nb/sr]	[nb/sr]
5.754	1.80	-0.9498	0.807	130.1 ± 6.8	53.4 ± 10.8	104.3 ± 17.2
5.614		-0.9498	0.796	150.5 ± 9.7		
4.238		-0.9498	0.608	134.7 ± 7.36		
3.401		-0.9498	0.359	130.3 ± 11.4		
5.614	1.85	-0.8562	0.781	150.1 ± 6.8	64.1 ± 12.1	99.3 ± 18.1
4.238		-0.8562	0.579	135.4 ± 6.4		
3.401		-0.8562	0.313	129.1 ± 10.6		
5.614	1.98	-0.6737	0.737	147.4 ± 5.8	50.9 ± 12.5	109.9 ± 21.4
4.238		-0.6737	0.494	135.1 ± 8.6		
5.614	2.08	-0.5716	0.696	137.2 ± 4.1	68.7 ± 6.8	89.3 ± 13.1
4.238		-0.5716	0.417	118.1 ± 6.0		

TABLE II: Systematic uncertainties for the E981-08 experiment.

Detector/Variable	Systematic Uncertainty (%)
Beam energy	0.12
A1 efficiency	0.57
Scintillator efficiencies	1.33
VDC efficiency	1.97
A2 efficiency	0.87
Charge	0.3
LH ₂ target density	0.2
Spectrometer acceptance	0.8
Background subtraction	0.3
Kaon absorption	0.1
Quadrature sum	2.8

[4]. [Note, using only [4] in fitting c_x gives a poor result showing the impact of the new data.] Results of the modified Regge model (fitRM) are shown in Figs. 3 and 4 by solid lines. The off-shell form factors provide both proper normalization and better energy dependence of the cross sections. The flatter Q^2 -dependence of σ_T is described by fitRM, especially for large Q^2 , but the known inability of RM to describe photoproduction cross sections below 3 GeV [16, 17] is shown by the photoproduction point in Fig. 3. The ratio σ_L/σ_T has the proper decreasing

Q^2 -dependence in fitRM like RM[6], although the ratio depends on the form factors now. Improvement in the energy dependence for both σ_T and σ_L is also apparent in Fig. 4.

In summary, new measurements of the longitudinal and transverse separated cross sections for the $^1\text{H}(e, e'K^+)\Lambda$ reaction at $Q^2 = 1.9$ and $2.35 \text{ GeV}/c^2$ have been obtained. These new data are in agreement with previous measurements and extend the region for which the separated cross sections are available. The data reveal a flat energy dependence for both longitudinal and transverse cross sections and put important constraints on models for kaon electroproduction.

Using the new and previous [4] data on the electroproduction of kaons we refined the Regge model by including phenomenological off-shell corrections.

Results show the reaction mechanism at forward kaon angles and non zero Q^2 can be described solely by the t-channel exchanges and that the off-shell form factors are important to describe the observed flat energy dependence, especially for σ_L . The used trajectory form factors, if interpreted as the form factors of the K^+ and K^* mesons, provide proper values of the mean-squared electromagnetic radii and the kaon form factor is consistent with the low- Q^2 data.

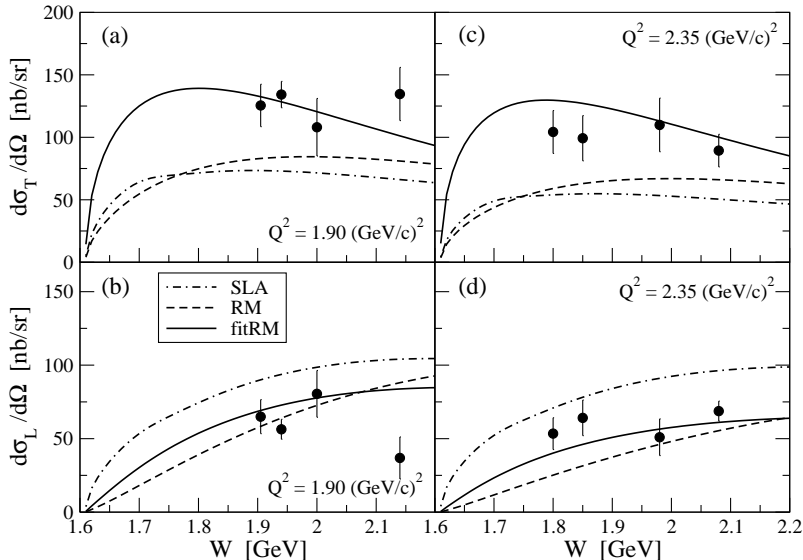


FIG. 4: Energy dependence of separated cross sections from this experiment in comparison with predictions of models as in Fig.3 for $Q^2 = 1.90$ GeV, (a) and (b), and 2.35 GeV, (c) and (d), and zero kaon angle.

We acknowledge the Jefferson Lab physics and accelerator Division staff for the outstanding efforts that made this work possible. This work was supported by U.S. DOE contract DE-AC05-84ER40150, Mod. nr. 175, under which the Southeastern Universities Research Association (SURA) operates the Thomas Jefferson National Accelerator Facility, by the Italian Istituto Nazionale di Fisica Nucleare and by the Grant Agency of the Czech Republic under grant No. 202/08/0984, and by the U.S. DOE under contracts, DE-AC02-06CH11357, DE-FG02-99ER41065, and DE-AC02-98-CH10886.

[1] R.P. Feynman, *Photon Hadron Interactions*, Benjamin Inc., (1972).
[2] F. Halzen and A. Martin, *Quarks and Leptons: An Introductory Course in Modern Particle Physics*, John Wiley & Sons Inc., (1984).
[3] P. Ambrozewicz *et al.*, Phys. Rev. C **75**, 045203 (2007).
[4] R.M. Mohring *et al.*, Phys. Rev. C **67**, 055205 (2003).
[5] T. Mizutani, C. Fayard, G.-H. Lamot, and B. Saghai, Phys. Rev. C **58**, 75 (1998); J.C. David, C. Fayard, G.H. Lamot, and B. Saghai, Phys. Rev. C **53**, 2613 (1996).

[6] M. Guidal, J.-M. Laget, and M. Vanderhaeghen, Nucl. Phys. A **627**, 645 (1997); Phys. Rev. C **61**, 025204 (2000).
[7] P. Markowitz, M. Iodice, S. Frullani, C.C. Chang, O.K. Baker, spokesperson, *Jefferson Lab Experiment E98-108*, (1998).
[8] John Alcorn *et al.*, Basic Instrumentation for Hall A at Jefferson Lab, Nucl. Instrum. Methods A **522**, (2004).
[9] M. Coman. M.S. thesis, Florida International University (2000).
[10] L. Lagamba *et al.*, Nucl. Instrum. Methods A **471**, 325 (2001).
[11] P.E. Ulmer, MCEEP: Monte Carlo for electro-nuclear coincidence experiments, version 3.7, http://hallaweb.jlab.org/data_reduc/mc, (2002).
[12] P. Brauel, *et al.*, Z.Phys. C, **3** 101 (1979).
[13] J. Cha, Ph.D. dissertation, Hampton University, http://www1.jlab.org/ul/generic_reports/thesis.cfm (2000).
[14] M. Coman, Ph.D. dissertation, Florida International University (2005).
[15] A. Bleckmann, S. Herda, U. Opara, W. Schulz, W.J. Schuille, and H. Urbahn, Z. Phys. **239**, 1 (1970).
[16] R. Bradford *et al.*, Phys. Rev. C **73**, 035202 (2006).
[17] M. Sumihama *et al.*, Phys. Rev. C **73**, 035214 (2006).
[18] S.R. Amendolia *et al.*, Phys. Lett. B **178**, 435 (1986).